Coupled Systems Mechanics, *Vol. 8, No. 3 (2019) 259-271*
DOI: https://doi.org/10.12989/csm.2019.8.3.259

Forced vibration analysis of functionally graded sandwich deep beams

Şeref D. Akbaş*

Department of Civil Engineering, Bursa Technical University, Yıldırım Campus, Yıldırım, Bursa 16330, Turkey

(Received March 5, 2019, Revised March 29, 2019, Accepted March 30, 2019)

Abstract. This paper presents forced vibration analysis of sandwich deep beams made of functionally graded material (FGM) in face layers and a porous material in core layer. The FGM sandwich deep beam is subjected to a harmonic dynamic load. The FGM in the face layer is graded though the layer thickness. In order to get more realistic result for the deep beam problem, the plane solid continua is used in the modeling of The FGM sandwich deep beam. The equations of the problem are derived based the Hamilton procedure and solved by using the finite element method. The novelty in this paper is to investigate the dynamic responses of sandwich deep beams made of FGM and porous material by using the plane solid continua. In the numerical results, the effects of different material distributions, porosity coefficient, geometric and dynamic parameters on the dynamic responses of the FGM sandwich deep beam are investigated and discussed.

Keywords: sandwich composites; deep beam; forced vibration; porosity; functionally graded material

1. Introduction

Sandwich composites made of two thin face layers and thick core layer In a sandwich material, the thin layers are composed high strength materials and the core layer is composed lightweight materials. Sandwich composite structures are used in a lot of engineering applications such as aircrafts, civil and mechanical engineering projects.

Functionally graded material (FGM) is a type of composites whose composition vary though in a direction. In the last quarter century, the FGMs have been found in many engineering applications, such as aircrafts, space vehicles and biomedical sectors. Also, the FGMs are used as a part of sandwich composite structures.

Due to their low weight, high vibration dissipation, high electrical and thermal resistance and low cost, porous materials are often preferred in engineering applications. Especially, porous materials are preferred and designed in the core layers of the sandwich structures.

With increasing FGM sandwich structures, the more researchers have been investigated the mechanical studies of FGM sandwich structures in last decades. In the literature, some investigations of mechanical behavior of FGM sandwich structures are as follows; Bhangale and Ganesan (2006) analyzed stability and dynamic analysis of FGM sandwich beams with viscoelastic layer under

*Corresponding author, Ph.D., E-mail: serefda@yahoo.com

http://www.techno-press.org/?journal=csm&subpage=8 ISSN: 2234-2184 (Print), 2234-2192 (Online)

thermal effects by using finite element method. Zenkour *et al.* (2010) investigated bending results of FGM viscoelastic sandwich beams embedded elastic foundation. Wang and Shen (2011) analyzed nonlinear static and stability of FGM sandwich plates resting on foundation under thermal effects. Nguyen and Nguyen (2015) examined mechanical results of FGM sandwich beams by using a new higher-order shear deformation theory. Vo *et al.* (2015) analyzed static results of FGM sandwich beams by using a quasi-3D theory. Akbaş (2013) examined the effects of the cracks on the geometrically nonlinear static responses of FGM beams.

Bouakkaz *et al.* (2015) examined vibration of cracked FGM sandwich beam based on higher order beam theory. Chen *et al.* (2016) analyzed nonlinear vibration of sandwich beams with FGM porous core. Yahia *et al.* (2015) investigated wave propagation of FGM porous plates by using higher-order shear deformation theory. Akbaş (2016b) investigated forced vibration responses of nanobeams based coupled stress theory. Avcar (2015) investigated the vibration of non-homogeneous beams with considering rotary inertia effects. Tounsi *et al.* (2016) and Benbakhti *et al.* (2016) investigated buckling and vibration analysis of FGM sandwich plates by using higher order shear deformation theories. Ebrahimi and Farazamandnia (2017,2018) investigated thermo-mechanical and buckling analysis of sandwich beams with reinforced carbon nanotubes by using the ddifferential transform method . Akbaş (2017a, b, c, d) studied the porosity effects on the free vibration, post-buckling behavior of the FGM beams by using finite element method. Abdelaziz et a. (2017) studied free vibration of FGM sandwich plates considering with shear deformation. Avcar and Alwan (2017), Avcar and Mohammed (2018) investigated free vibration of FGM beams by analytically. Bennai *et al.* (2015) analyzed vibration and buckling of the FGM sandwich beams by analytically. Akbaş (2015a, b, 2016a) studied post-buckling analysis of FGM beams. Barka *et al.* (2016) presented thermal-postbuckling analysis of FGM sandwich plates embaded elastic foundation by using Galerkin method. Akbaş (2015c, 2017e, 2017, 2018d) analyzed dynamic responses of FGM beams. Van Tung (2017) presented nonlinear results of FGM sandwich panels embaded on foundation under thermal and external pressur effects. Akbaş (2018a) studied forced vibration of FGM deep beams with porosity by using finite element method based on plane solid continua model. Akbaş (2018b) investigated forced vibration responses of cracked FGM nono beams by using coupled stress theory. Akbaş (2018c) analyzed geometrically nonlinear static displacements of FGM porous beams by using finite element method based on total Lagrangian nonlinearity approach. Hadji *et al.* (2015, 2017, 2019), Zouatnia *et al.* (2017), Bourada *et al.* (2019) investigated the effects of the porosity on the free vibration responses of FGM beams by using the Navier method. Gholami and Ansari (2018) studied nonlinear vibration of FGM plates with graphane platelet. Civalek and Baltacıoğlu (2019) analyzed vibration of laminated FGM annular plates.

It is seen from literature, dynamic investigation of FGM sandwich deep beam has not been investigated by using plane solid continua so far. The primary purpose of this study is to fill this gap for FGM sandwich deep beams. In this paper, forced vibration analysis of FGM sandwich deep beams with porous core is presented under a harmonic dynamic load. The face layers and core materials of sandwich deep beams are considered as FGM and porous materials, respectively. The governing equations of problem are obtained by using the Hamilton principle and solved by finite element method. The plane solid continua model is used in the FGM sandwich deep beam. The novelty in this paper is to investigate the dynamic responses of sandwich deep beams made of FGM and porous material by using the plane solid continua. In a recent study, Akbaş (2018a) investigated the dynamic analysis of FGM porous deep beams by using the plane solid continua model. The distinctive feature of this study is using and developing the plane solid continua model for

sandwich FGM deep beams with porous core material. In the results, the effects of different material distributions, porosity geometry and dynamic parameters on the dynamic responses of FGM deep beam are investigated.

2. Theory and formulation

A simply supported FGM sandwich deep beam with porous core under dynamically point load P(t) at the midpoint of the beam is displayed in Fig. 1. The height of the face layer layers are h_1 and the height of the core layer is h_2. The face layer is considered as FGM material and the core material has porous property. In Fig. 1, L, b, h are the length, width and height of the beam, respectively.

In the face layer, material properties change though the height direction. The material distribution of face layer (P_f) is varied as a power-law function

$$P_f(Y) = \left(P_{fT} - P_{fB}\right)\left(\frac{Y}{h_1} + \frac{1}{2}\right)^n + P_{fB} \tag{1}$$

where P_{fT} and P_{fB} are top and bottom properties of the FGM face layer, n is the material distribution coefficient. The FGM face layers becomes a fully top surface material as n=0. The core layer is considered as a porous material and its effective material property (P_c) is selected in the even porosity distribution

$$P_c(a) = P_c(1 - a) \tag{2}$$

where a (a<<1) is the volume fraction of porosities in the core layer. When a=0 , the beam becomes perfect. In the even porosity distribution, the voids stack uniformly in the whole area of the material.

In the solution of the sandwich deep beam problem, the plane model is used in order to obtain more realistic results. For plane solid continua model, the strain- displacement relations are given as

$$\varepsilon_{XX} = \frac{\partial u}{\partial X}, \quad \varepsilon_{YY} = \frac{\partial v}{\partial Y}, \qquad 2\varepsilon_{XY} = \frac{\partial u}{\partial Y} + \frac{\partial v}{\partial X} \tag{3}$$

where u, v are displacements in the X and Y directions respectively. ε_{XX} and ε_{YY} are normal strains and ε_{XY} is shear strain. The strain- displacement formulas are given in matrix format as follows

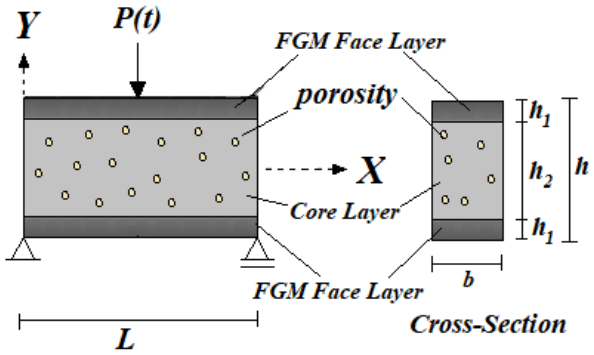

Fig. 1 A simply supported sandwich deep beam with FGM face layer and porous core layer under dynamic point load

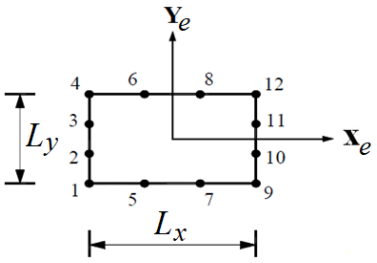

Fig. 2 Twelve-node plane element.

$$\begin{Bmatrix} \varepsilon_{XX} \\ \varepsilon_{YY} \\ 2\varepsilon_{XY} \end{Bmatrix} = \begin{bmatrix} \frac{\partial}{\partial X} & 0 \\ 0 & \frac{\partial}{\partial Y} \\ \frac{\partial}{\partial Y} & \frac{\partial}{\partial X} \end{bmatrix} \begin{Bmatrix} u \\ v \end{Bmatrix} \tag{4}$$

$$\{\varepsilon\} = [D]\{d\} \tag{5}$$

where$[D]$is the differential operator between deformation and displacement, $\{d\}$ is the displacement vector. The stress-strain relation of the face layer is given as follows

$$\begin{Bmatrix} \sigma_{XX} \\ \sigma_{YY} \\ \sigma_{XY} \end{Bmatrix}^f = \begin{bmatrix} C_{11}^f(Y) & C_{12}^f(Y) & 0 \\ C_{12}^f(Y) & C_{22}^f(Y) & 0 \\ 0 & 0 & C_{66}^f(Y) \end{bmatrix} \begin{Bmatrix} \varepsilon_{XX} \\ \varepsilon_{YY} \\ 2\varepsilon_{XY} \end{Bmatrix} \tag{6a}$$

$$\{\sigma\}^f = [C]^f\{\varepsilon\} \tag{6b}$$

The stress-strain relation of the core layer is given as follows

$$\begin{Bmatrix} \sigma_{XX} \\ \sigma_{YY} \\ \sigma_{XY} \end{Bmatrix}^c = \begin{bmatrix} C_{11}^c(a) & C_{12}^c(a) & 0 \\ C_{12}^c(a) & C_{22}^c(a) & 0 \\ 0 & 0 & C_{66}^c(T,a) \end{bmatrix} \begin{Bmatrix} \varepsilon_{XX} \\ \varepsilon_{YY} \\ 2\varepsilon_{XY} \end{Bmatrix} \tag{7a}$$

$$\{\sigma\}^c = [C]^c\{\varepsilon\} \tag{7b}$$

where $[C]^f$ and $[C]^c$ are the reduced constitutive tensor of face and core layers, respectively and theirs components are given as follows

$$\begin{gathered} C_{11}^f(Y) = C_{22}^f(Y) = \frac{E(Y)}{1-\nu(Y)^2},\ C_{66}^f(Y) = \frac{E(Y)}{2(1+\nu(Y))} \\ C_{21}^f(Y) = C_{21}^f(Y) = \nu(Y)\frac{E(Y)}{1-\nu(Y)^2}, \end{gathered} \tag{8a}$$

$$\begin{gathered} C_{11}^c(a) = C_{22}^c(a) = \frac{E(a)}{1-\nu(a)^2},\ C_{66}^c(a) = \frac{E(a)}{2(1+\nu(a))} \\ C_{12}^c(a) = C_{21}^c(a) = \nu(a)\frac{E(a)}{1-\nu(a)^2}, \end{gathered} \tag{8b}$$

In the deriving of the governing equations, the Hamilton's procedure is used. The virtual work equation of the plane solid continua model with dynamic effect is given as follows

$$\int_A (\sigma_{XX}\delta\varepsilon_{XX} + 2\sigma_{XY}\delta\varepsilon_{XY} + \sigma_{YY}\delta\varepsilon_{YY} + \rho(Y,a)\ddot{u}\delta u + \rho(Y,a)\ddot{v}\delta v)d - b\int_S (r_X\delta u + r_Y\delta v)dS - b\int_A (k_X\delta u + k_Y\delta v)\,dA = 0 \tag{9}$$

ρ is the mass density, r_X and r_Y are the boundary forces in the X and Y directions respectively. k_X and k_Y are the body forces in the X and Y directions respectively. In Eq. (8), $\ddot{u}$ and $\ddot{v}$ indicate the second derivative with respect to time. In the finite element solution, Twelve-node plane element is used as shown in Fig. 2.

In Fig. 2, L_x and L_y indicate the finite element length in the X and Y directions, respectively. The displacement vector with the node displacements are given as follows

$$\{d\} = [\emptyset]\{d_n\} \tag{10}$$

where $[\emptyset]$ is the shape function and $\{d_n\}$ is the node displacement vector

$$[\emptyset] = [\emptyset_1\ \emptyset_2 \ldots . \emptyset_{12}] \tag{11}$$

$$\{d_n\}^T = \{u_1 \quad u_2 \quad \ldots \quad u_{12} \quad v_1 \quad v_2 \quad \cdots \quad v_{12}\} \tag{12}$$

where u_i and v_i are horizontal and vertical displacements in the nodes, respectively. The shape functions for twelve-node plane element are given according to local element coordinates X_e and Y_e as follows

$$\begin{aligned}
\emptyset_1 &= \frac{1}{32}\left(1-\frac{2X_e}{L_x}\right)\left(1-\frac{2Y_e}{L_y}\right)\left(-10+9\left(\frac{4X_e{}^2}{L_x{}^2}+\frac{4Y_e{}^2}{L_y{}^2}\right)\right),\\
\emptyset_2 &= \frac{9}{32}\left(1-\frac{2X_e}{L_x}\right)\left(1-\frac{4Y_e{}^2}{L_y{}^2}\right)\left(1-\frac{6Y_e}{L_y}\right),\\
\emptyset_3 &= \frac{9}{32}\left(1-\frac{2X_e}{L_x}\right)\left(1-\frac{4Y_e{}^2}{L_y{}^2}\right)\left(1+\frac{6Y_e}{L_y}\right),\\
\emptyset_4 &= \frac{1}{32}\left(1-\frac{2X_e}{L_x}\right)\left(1+\frac{2Y_e}{L_y}\right)\left(-10+9\left(\frac{4X_e{}^2}{L_x{}^2}+\frac{4Y_e{}^2}{L_y{}^2}\right)\right),\\
\emptyset_5 &= \frac{9}{32}\left(1-\frac{2Y_e}{L_y}\right)\left(1-\frac{4X_e{}^2}{L_x{}^2}\right)\left(1-\frac{6X_e}{L_x}\right),\\
\emptyset_6 &= \frac{9}{32}\left(1+\frac{2Y_e}{L_y}\right)\left(1-\frac{4X_e{}^2}{L_x{}^2}\right)\left(1-\frac{6X_e}{L_x}\right),\\
\emptyset_7 &= \frac{9}{32}\left(1-\frac{2Y_e}{L_y}\right)\left(1-\frac{4X_e{}^2}{L_x{}^2}\right)\left(1+\frac{6X_e}{L_x}\right),\\
\emptyset_8 &= \frac{9}{32}\left(1+\frac{2Y_e}{L_y}\right)\left(1-\frac{4X_e{}^2}{L_x{}^2}\right)\left(1+\frac{6X_e}{L_x}\right),\\
\emptyset_9 &= \frac{1}{32}\left(1+\frac{2X_e}{L_x}\right)\left(1-\frac{2Y_e}{L_y}\right)\left(-10+9\left(\frac{4X_e{}^2}{L_x{}^2}+\frac{4Y_e{}^2}{L_y{}^2}\right)\right),\\
\emptyset_{10} &= \frac{9}{32}\left(1+\frac{2X_e}{L_x}\right)\left(1-\frac{4Y_e{}^2}{L_y{}^2}\right)\\
\emptyset_{11} &= \frac{9}{32}\left(1+\frac{2X_e}{L_x}\right)\left(1-\frac{4Y_e{}^2}{L_y{}^2}\right)\left(1+\frac{6Y_e}{L_y}\right),\\
\emptyset_{12} &= \frac{1}{32}\left(1+\frac{2X_e}{L_x}\right)\left(1+\frac{2Y_e}{L_y}\right)\left(-10+9\left(\frac{4X_e{}^2}{L_x{}^2}+\frac{4Y_e{}^2}{L_y{}^2}\right)\right)
\end{aligned} \tag{13}$$

Substituting Eqs. (10)-(13) into Eq. (9), the virtual work equation can be rewritten as follows

$$b\int_A \{\delta d_n\}^T\left([B]^T[C][B]\{d_n\}+\rho(Y,a)[\emptyset]^T[\emptyset]\{\delta\ddot{d}\}\right)dA$$
$$-b\int_S \{\delta d_n\}^T[\emptyset]^T\begin{Bmatrix}r_X\\r_Y\end{Bmatrix}dS-b\int_A \{\delta d_n\}^T[\emptyset]^T\begin{Bmatrix}k_X\\k_Y\end{Bmatrix}dA=0 \tag{14a}$$

$$\{\delta d_n\}^T\left([K]\{d_n\}+[M]\{\ddot{d}\}-\{r\}-\{s\}\right)=0 \tag{14b}$$

By using Eq. (14), the equation of motion can be obtained as follows

$$[K]\{d_n\}+[M]\{\ddot{d_n}\}=\{F\} \tag{15}$$

where $[K]$ is the element stiffness matrix, $[M]$ is the element mass matrix, $\{F\}$ is the load vector, $\{d_n\}$ is the displacement vector, $\{\ddot{d_n}\}$ is the acceleration vector, $\{s\}$ is the body force vector, $\{r\}$ is the surface load vector. The details of components of the finite element equation are given as follows

$$[K]=b\int_A [B]^T[C][B]dA \tag{16a}$$

$$[M]=b\int_A \rho(Y,a)[\emptyset]^T[\emptyset]dA \tag{16b}$$

$$\{F\}=\{r\}+\{s\} \tag{16c}$$

$$\{r\}=\int_S [\emptyset]^T\begin{Bmatrix}r_X\\r_Y\end{Bmatrix}dS \tag{16d}$$

$$\{s\}=\int_A [\emptyset]^T\begin{Bmatrix}k_X\\k_Y\end{Bmatrix}dA \tag{16e}$$

The dynamic point load is considered as a harmonic function as follows

$$P(t)=P_0\sin(\bar{w}t) \tag{17}$$

where P_0 is the amplitude of the dynamic load and $\bar{w}$ is the frequency of the dynamic load. In the solution of the forced vibration problem, the displacement vector is assumed as following form

$$\{d_n\}=\{d_m\}\sin(\bar{w}t) \tag{18}$$

where $\{d_m\}$ is the amplitude of the displacements. The equation of motion can be obtained as follows

$$\{d_m\}([K]-\bar{w}^2[M])=\{F\} \tag{19}$$

3. Numerical results

In the numerical results, the effects of material distribution (n), the volume fraction of porosity (a), the frequency of the dynamic load ($\bar{w}$) and the aspect ratio (L/h) on the forced vibration

responses of the FGM sandwich deep beam with porous core are investigated. In the materials of FGM face layer, the materials of top and bottom surfaces are considered as Zirconia and Aluminium, respectively. The material properties of Zirconia are E=151 GPa, $\nu = 0.3$, $\rho = 3000\ kg/m^3$ and Aluminium's properties are E=70 GPa, $\nu = 0.32$, $\rho = 2710\ kg/m^3$. The FGM face layers are graded according to a power-law function that gives in equation 1. The geometry values of the FGM sandwich deep beam are considered as follows: b = 0.3 m, h = 0.5 m. The aspect ratio is taken as L/h=2 in the numerical study, unless otherwise stated.

The numbers of the finite element in both X and Y directions are chosen to be equal because of the deep beam geometry. The finite element number in both X and Y directions is taken as 20. The finite element number of FGM face layer is taken as 8. In the finite element assembly procedure, the material properties of each finite elements is calculated and selected according to layer position. In the implementation of the boundary conditions, the lower left-hand corner in the beam is selected pinned support and the lower right-hand corner in the beam is selected roller support.

Fig. 3 shows the effect of the material distribution parameter *(n)* on the dimensionless maximum vertical displacements (v/L) at the middle of the beam of the porous functionally graded deep beam is presented for different the volume fraction of porosity (a) for $P_0 = 10000\ kN$ and $\overline{w}$=200 *rd/sn*. It is seen from fig. 3 that the dimensionless displacements increase with increasing n parameter because the stiffness of the beam decrease according to the material distribution in equation 1. It is noted that the Young modulus of Aluminium is smaller than Zirconia. With increasing n parameter, the FGM face layer gets to fully Aluminium. Hence, the strength of the beam decreases with increasing the n parameter. It can be seen from Fig. 3 that the difference among of porosity parameters increases significantly because of increasing n parameter. Also, increasing the porosity in core layer yields to an increasing displacements because the strength of the material decrease with the porosity. The effect of the FGM material distribution on time- dimensionless displacements relation is presented in Fig. 4. In this figure, the time responses of FGM sandwich deep beam with porous core are plotted for different n and porosity parameters a for $P_0 = 1000\ kN$ and $\overline{w}$=3 *rd/sn*. It is seen from Figs. 3 and 4 that the material distribution parameters change the effects the porosity on the deep beam considerably.

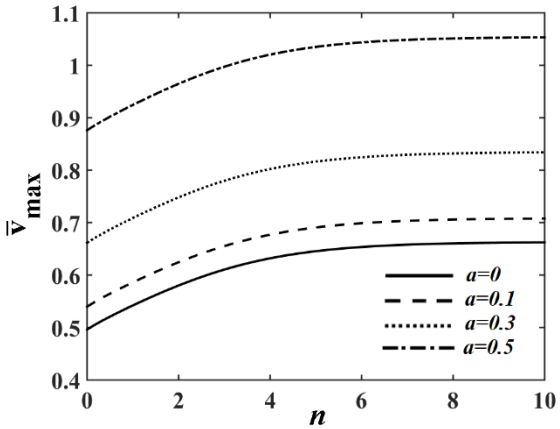

Fig. 3 The effects of the material distribution parameter n on the dimensionless maximum vertical displacements for different porosity coefficients

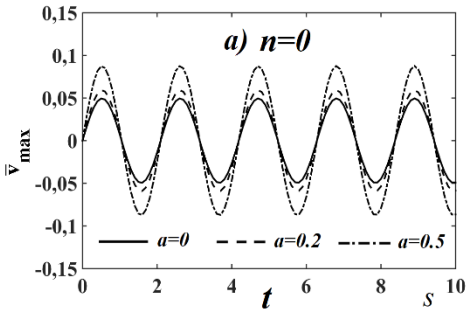

(a) For n=0 (b) For n=0.5

(c) For n=2

Fig. 4 Time responses of the FGM sandwich deep beam for different n and a values

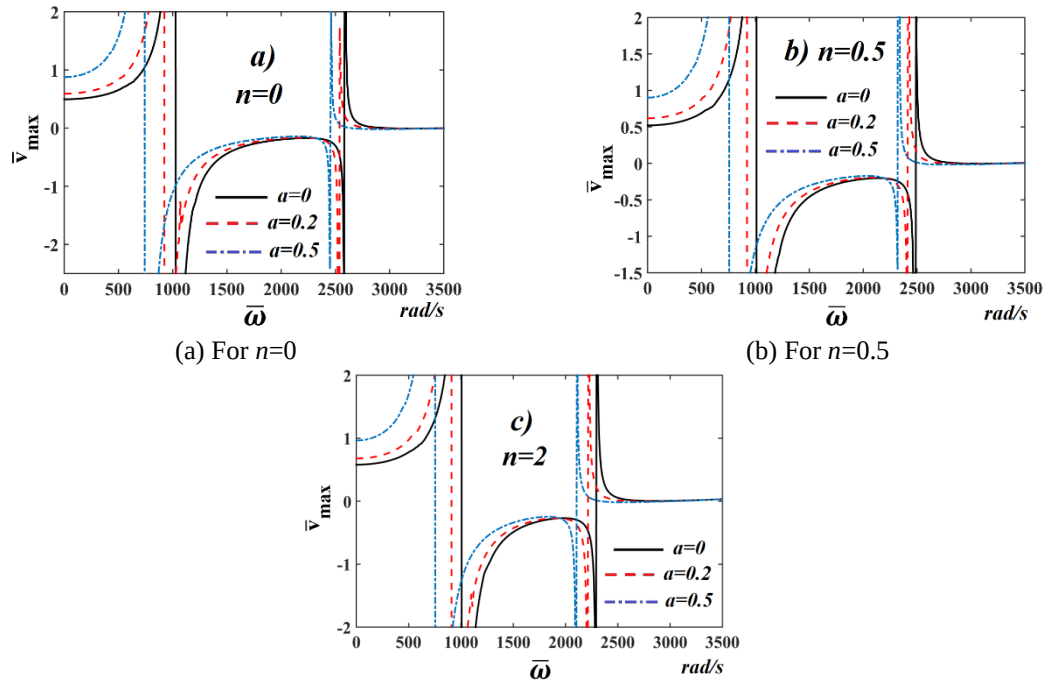

(a) For n=0 (b) For n=0.5

(c) For n=2

Fig. 5 The relationship between of the dimensionless maximum vertical displacements and the frequency of the dynamic load ($\bar{w}$) for different n and a values

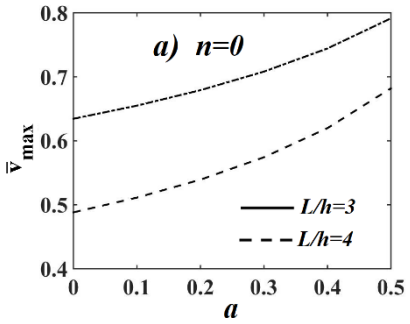

(a) For n=0

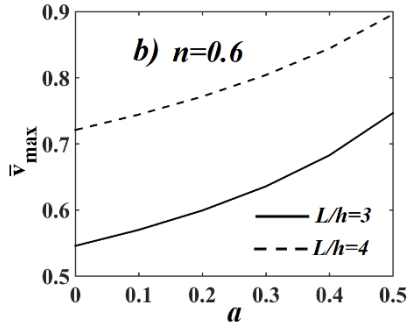

(b) For n=0.5

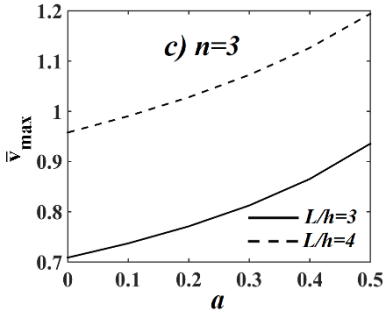

(c) For n=2

Fig. 6 The effects of the aspect ratio on the dimensionless maximum vertical displacements for different n and a values

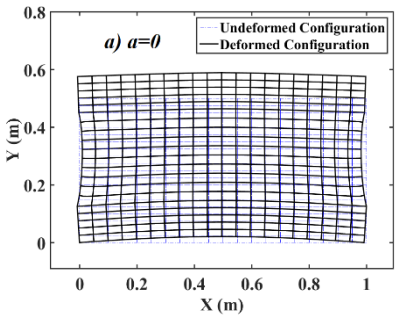

(a) For a=0

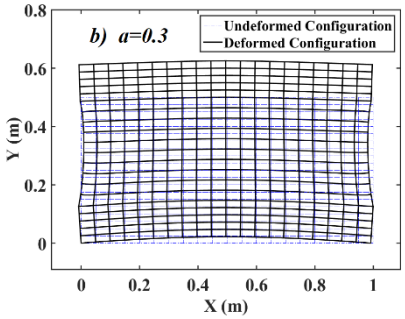

(b) For a=0.3

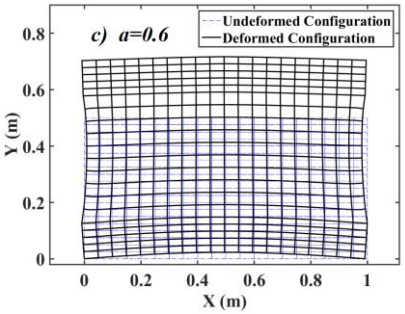

(c) For a=0.6

Fig. 7 The deformed configurations of the FGM sandwich deep beam for different porosity coefficients

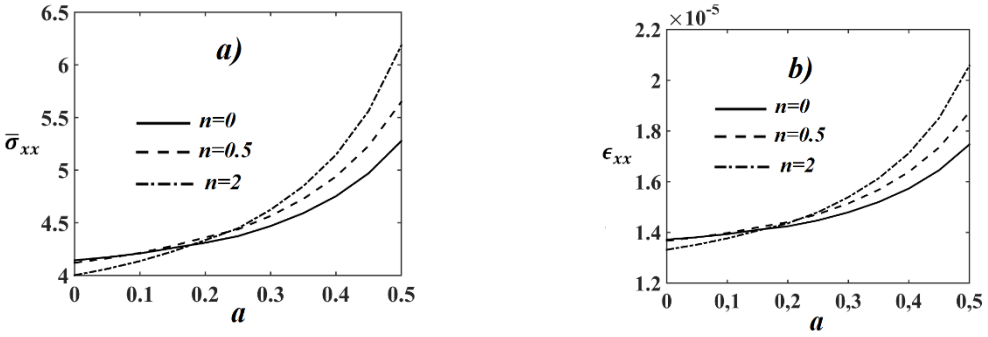

(a) For the dimensionless stress (b) For strain

Fig. 8 The effects of the porosity coefficient on the dimensionless stress and strain at *X*=*L*/2, *Y*=-0.5h for different *n* parameter

In Fig. 5, the frequency of the dynamic load ($\bar{w}$)-dimensionless maximum vertical displacements relation is presented for different values of FGM material distribution parameters for $P_0 = 10000\ kN$. As seen from Fig. 5, the resonance points, where the frequency of the dynamic load ($\bar{w}$) and the fundamental frequency of the beam is equal, decrease dramatically with increasing in both porosity and FGM material distribution parameters. The reason of this situation is the rigidity of the sandwich deep beam decrease with increasing in *n* and *a* parameters. So, the resonance frequency decreases naturally. It shows that the material distribution and porosity parameters are very effective in the forced vibration responses.

In Fig. 6, the effect of the aspect ratios (*L/h*) on the dynamic displacements is presented for different of porosity and *n* parameters for $P_0 = 10000\ kN$ and $\bar{w}$=100 *rd/sn*. The effect of the porosity coefficient on the dynamic responses increases with increasing the aspect ratio as seen in Fig. 6. Also, The difference among the results of the porosity parameters increases with increasing the *n* parameter. In higher values of aspect ratio, the porosity and material distribution parameter are very effective on the dynamic responses of the FGM sandwich beam.

Fig. 7 shows that the deformed configuration of the FGM sandwich deep beam with different values of the porosity parameters for *n*=0.5, $P_0 = 1000\ kN$ and $\bar{w}$=200 *rd/sn*. It is seen from Fig. 7 that the displacements increase significantly with increasing porosity.

In Fig. 8, the effects of the n and a parameters on the stress and strain are presented. In Fig. 8, the dimensionless normal stress ($\bar{\sigma}_{xx} = \sigma_{xx} bh^2/P_0 L$) and normal strain calculated and presented at *X*=*L*/2, *Y*=-0.5h for different values *a* and *n* parameter for $P_0 = 10\ kN$, *L/h*=3.5 and $\bar{w}$=1000 *rd/sn*. It is seen from fig. 8 that variation of *n* and *a* affect the stress and strain considerably. The *n* parameter changes the stress and strain values significantly. The effect of porosity varies considerably with increasing in *n* parameter

4. Conclusions

The forced vibration analysis of FGM sandwich deep beams with porous core is investigated under a harmonic dynamic load by using the finite element method. The face layers are considered as FGM and the core layer is considered a porous material. In the FGM distribution, the power-law function is used. In the modelling of the FGM sandwich deep beam, the plane solid continua model

is used. The effects of different material distributions, porosity geometry and dynamic parameters on the dynamic responses of FGM deep beam are investigated. It is observed from the results that the material distribution and the aspect ratio have important role on the effects the porosity on the dynamic responses of the FGM deep beams. With increasing in aspect ratio, the porosity and material distribution parameter gain importance in the dynamic responses of the porous sandwich deep beam. Also, the porosity change the resonance phenomena of the FGM sandwich deep beams significantly.

References

Abdelaziz, H.H., Meziane, M.A.A., Bousahla, A.A., Tounsi, A., Mahmoud, S.R. and Alwabli, A.S. (2017), "An efficient hyperbolic shear deformation theory for bending, buckling and free vibration of FGM sandwich plates with various boundary conditions", *Steel Compos. Struct.*, **25**(6), 693-704. https://doi.org/10.12989/scs.2017.25.6.693.

Akbaş, Ş.D. (2013), "Geometrically nonlinear static analysis of edge cracked Timoshenko beams composed of functionally graded material", *Math. Prob. Eng.*, http://dx.doi.org/10.1155/2013/871815.

Akbaş, Ş.D. (2015a), "Post-buckling analysis of axially functionally graded three-dimensional beams", *Int. J. Appl. Mech.*, **7**(03), 1550047. https://doi.org/10.1142/S1758825115500477.

Akbaş, Ş.D. (2015b), "On post-buckling behavior of edge cracked functionally graded beams under axial loads", *Int. J. Struct. Stability Dyn.*, **15**(04), 1450065. https://doi.org/10.1142/S0219455414500655.

Akbaş, Ş.D. (2015c), "Wave propagation of a functionally graded beam in thermal environments", *Steel Compos. Struct.*, **19**(6), 1421-1447. https://doi.org/10.12989/scs.2015.19.6.1421.

Akbaş, Ş.D. (2016a), "Post-buckling analysis of edge cracked columns under axial compression loads", *Int. J. Appl. Mech.*, **8**(8), 1650086. https://doi.org/10.1142/S1758825116500861.

Akbaş, Ş.D. (2016b), "Forced vibration analysis of viscoelastic nanobeams embedded in an elastic medium", *Smart Struct. Syst.*, **18**(6), 1125-1143. https://doi.org/10.12989/sss.2016.18.6.1125.

Akbaş, Ş.D. (2017a), "Nonlinear static analysis of functionally graded porous beams under thermal effect", *Coupled Syst. Mech.*, **6**(4), 399-415. https://doi.org/10.12989/csm.2017.6.4.399.

Akbas, Ş.D. (2017b), "Post-buckling responses of functionally graded beams with porosities", *Steel Compos. Struct.*, **24**(5), 579-589. https://doi.org/10.12989/scs.2017.24.5.579.

Akbaş, Ş.D. (2017c), "Vibration and static analysis of functionally graded porous plates", *J. Appl. Comput. Mech.*, **3**(3), 199-207. https://dx.doi.org/10.22055/jacm.2017.21540.1107.

Akbaş, Ş.D. (2017d), "Thermal effects on the vibration of functionally graded deep beams with porosity", *Int. J. Appl. Mech.*, **9**(05), 1750076. https://doi.org/10.1142/S1758825117500764.

Akbaş, Ş.D. (2017e), "Forced vibration analysis of functionally graded nanobeams", *Int. J. Appl. Mech.*, **9**(07), 1750100. https://doi.org/10.1142/S1758825117501009.

Akbaş, Ş.D. (2017f), "Free vibration of edge cracked functionally graded microscale beams based on the modified couple stress theory", *Int. J. Struct. Stability Dyn.*, **17**(03), 1750033. https://doi.org/10.1142/S021945541750033X.

Akbaş, Ş.D. (2018a), "Forced vibration analysis of functionally graded porous deep beams", *Compos. Struct.*, **186**, 293-302. https://doi.org/10.1016/j.compstruct.2017.12.013.

Akbas, Ş.D. (2018b), "Forced vibration analysis of cracked functionally graded microbeams", *Adv. Nano Res.*, **6**(1), 39-55. https://doi.org/10.12989/anr.2018.6.1.39.

Akbas, Ş.D. (2018c), "Geometrically nonlinear analysis of functionally graded porous beams", *Wind Struct.*, **27**(1), 59-70. https://doi.org/10.12989/was.2018.27.1.59.

Akbas, Ş.D. (2018d), "Investigation on free and forced vibration of a bi-material composite beam", *J. Polytechnic-Politeknik Dergisi*, **21**(1), 65-73.

Avcar, M. (2015), "Effects of rotary inertia shear deformation and non-homogeneity on frequencies of beam",

Struct. Eng. Mech., **55**(4), 871-884. https://doi.org/10.12989/sem.2015.55.4.871.
Avcar, M. and Alwan, H.H.A. (2017), "Free vibration of functionally graded Rayleigh beam", *Int. J. Eng. Appl. Sci.*, **9**(2), 127-137. http://dx.doi.org/10.24107/ijeas.322884.
Avcar, M. and Mohammed, W.K.M. (2018), "Free vibration of functionally graded beams resting on Winkler-Pasternak foundation", *Arab. J. Geosci.*, **11**(10), 232. https://doi.org/10.1007/s12517-018-3579-2.
Barka, M., Benrahou, K. H., Bakora, A. and Tounsi, A. (2016), "Thermal post-buckling behavior of imperfect temperature-dependent sandwich FGM plates resting on Pasternak elastic foundation", *Steel Compos. Struct.*, **22**(1), 91-112. https://doi.org/10.12989/scs.2016.22.1.91.
Benbakhti, A., Bouiadjra, M. B., Retiel, N. and Tounsi, A. (2016), "A new five unknown quasi-3D type HSDT for thermomechanical bending analysis of FGM sandwich plates", *Steel Compos. Struct.*, **22**(5), 975-999. https://doi.org/10.12989/scs.2016.22.5.975.
Bennai, R., Atmane, H.A. and Tounsi, A. (2015), "A new higher-order shear and normal deformation theory for functionally graded sandwich beams", *Steel Compos. Struct.*, **19**(3), 521-546. https://doi.org/10.12989/scs.2015.19.3.521.
Bhangale, R.K. and Ganesan, N. (2006), "Thermoelastic buckling and vibration behavior of a functionally graded sandwich beam with constrained viscoelastic core", *J. Sound Vib.*, **295**(1-2), 294-316. https://doi.org/10.1016/j.jsv.2006.01.026.
Bouakkaz, K., Hadji, L., Zouatnia, N. and Bedia E.A.A. (2015), "An analytical method for free vibration analysis of functionally graded sandwich beams", *Wind Struct.*, **23**(1), 59-73. https://doi.org/10.12989/was.2015.23.1.59.
Bourada, F., Bousahla, A.A., Bourada, M., Azzaz, A., Zinata, A. and Tounsi, A. (2019), "Dynamic investigation of porous functionally graded beam using a sinusoidal shear deformation theory", *Wind Struct.*, **28**(1), 19-30. https://doi.org/10.12989/was.2019.28.1.19.
Chen, D., Kitipornchai, S. and Yang, J. (2016), "Nonlinear free vibration of shear deformable sandwich beam with a functionally graded porous core", *Thin-Walled Struct.*, **107**, 39-48. https://doi.org/10.1016/j.tws.2016.05.025.
Civalek, Ö. and Baltacıoğlu, A.K. (2019), "Free vibration analysis of laminated and FGM composite annular sector plates", *Compos. Part B Eng.*, **157**, 182-194. https://doi.org/10.1016/j.compositesb.2018.08.101.
Ebrahimi, F. and Farazmandnia, N. (2017), "Thermo-mechanical analysis of carbon nanotube-reinforced composite sandwich beams", *Coupled Syst. Mech.*, **6**(2), 207-227. https://doi.org/10.12989/csm.2017.6.2.207.
Ebrahimi, F. and Farazmandnia, N. (2018), "Thermal buckling analysis of functionally graded carbon nanotube-reinforced composite sandwich beams", *Steel Compos. Struct.*, **27**(2), 149-159. https://doi.org/10.12989/scs.2018.27.2.149.
Gholami, R. and Ansari, R. (2018), "Nonlinear harmonically excited vibration of third-order shear deformable functionally graded graphene platelet-reinforced composite rectangular plates", *Eng. Struct.*, **156**, 197-209. https://doi.org/10.1016/j.engstruct.2017.11.019.
Hadji, L., and Adda Bedia, E.A. (2015), "Influence of the porosities on the free vibration of FGM beams", *Wind Struct.*, **21**(3), 273-287. https://doi.org/10.12989/was.2015.21.3.273.
Hadji, L., Zouatnia, N. and Bernard, F. (2019), "An analytical solution for bending and free vibration responses of functionally graded beams with porosities: Effect of the micromechanical models", *Struct. Eng. Mech.*, **69**(2), 231-241. https://doi.org/10.12989/sem.2019.69.2.231.
Hadji, L., Zouatnia, N. and Kassoul, A. (2017), "Wave propagation in functionally graded beams using various higher-order shear deformation beams theories", *Struct. Eng. Mech.*, **62**(2), 143-149. https://doi.org/10.12989/sem.2017.62.2.143.
Nguyen, T.K. and Nguyen, B.D. (2015), "A new higher-order shear deformation theory for static, buckling and free vibration analysis of functionally graded sandwich beams", *J. Sandw. Struct. Mater.*, **17**(6), 613-631. https://doi.org/10.1177%2F1099636215589237.
Tounsi, A., Houari, M.S.A. and Bessaim, A. (2016), "A new 3-unknowns non-polynomial plate theory for buckling and vibration of functionally graded sandwich plate", *Struct. Eng. Mech.*, **60**(4), 547-565. https://doi.org/10.12989/sem.2016.60.4.547.

Van Tung, H. (2017), "Nonlinear thermomechanical response of pressure-loaded doubly curved functionally graded material sandwich panels in thermal environments including tangential edge constraints", *J. Sandw. Struct. Mater.*, **20**(8), 974-1008. https://doi.org/10.1177%2F1099636216684312.

Vo, T.P., Thai, H.T., Nguyen, T.K., Inam, F. and Lee, J. (2015), "Static behaviour of functionally graded sandwich beams using a quasi-3D theory", *Compos. Part B Eng.*, **68**, 59-74. https://doi.org/10.1016/j.compositesb.2014.08.030.

Wang, Z.X. and Shen, H.S. (2011), "Nonlinear analysis of sandwich plates with FGM face sheets resting on elastic foundations", *Compos. Struct.*, **93**(10), 2521-2532. https://doi.org/10.1016/j.compstruct.2011.04.014.

Yahia, S.A., Atmane, H.A., Houari, M.S.A. and Tounsi, A. (2015), "Wave propagation in functionally graded plates with porosities using various higher-order shear deformation plate theories", *Struct. Eng. Mech.*, **53**(6), 1143-1165. https://doi.org/10.12989/sem.2015.53.6.1143.

Zenkour, A.M., Allam, M.N.M. and Sobhy, M. (2010), "Bending analysis of FG viscoelastic sandwich beams with elastic cores resting on Pasternak's elastic foundations", *Acta Mechanica*, **212**(3-4), 233-252. https://doi.org/10.1007/s00707-009-0252-6.

Zouatnia, N., Hadji, L. and Kassoul, A. (2017), "An analytical solution for bending and vibration responses of functionally graded beams with porosities", *Wind Struct.*, **25**(4), 329-342. https://doi.org/10.12989/was.2017.25.4.329.

CC